Interhemispheric thermal gradient and tropical Pacific climate

John C. H. Chiang,[1] Yue Fang,[1] and P. Chang[2]

[1] We explore the impact of interhemispheric thermal gradients forcing on the tropical Pacific ocean-atmosphere climate in an intermediate coupled model. The equatorial zonal sea surface temperature (SST) gradient strengthens with an increased northward interhemispheric thermal gradient, the increase arising from earlier onset and later retreat of the seasonal cold tongue, and intensification during the peak cold season. When the mean interhemispheric thermal gradient is reversed, the central equatorial Pacific SST annual cycle abruptly reverses in phase, with its cold season in Mar–May rather than Sep–Nov. While startling, this response is consistent with a prevailing hypothesis that ties the cold tongue SST annual cycle phase to the hemispheric mean asymmetry of the Intertropical Convergence Zone. El Niño-Southern Oscillation activity is also sensitive to the interhemispheric thermal gradient, with peak activity occurring when the mean gradient is small, reducing rapidly as the mean gradient increases in either direction. **Citation:** Chiang, J. C. H., Y. Fang, and P. Chang (2008), Interhemispheric thermal gradient and tropical Pacific climate, *Geophys. Res. Lett.*, *35*, L14704, doi:10.1029/2008GL034166.

1. Introduction

[2] Interhemispheric thermal gradients – i.e., the temperature contrast between the northern and southern hemispheres – have been implicated in paleoclimate scenarios to explain links between high latitude and tropical climate change [e.g., *Koutavas and Lynch-Stieglitz*, 2004]. Modeling studies have shown that the meridional position of the Intertropical Convergence Zone (ITCZ) is sensitive to interhemispheric thermal gradients [*Broccoli et al.*, 2006; *Chiang and Bitz*, 2005], shifting southwards to imposed cooling in the northern extratropics. However, the coupled tropical Pacific response to changing interhemispheric gradients has yet to be systematically explored, despite interhemispheric gradients being central to prevailing hypotheses of the tropical Pacific annual cycle [*Mitchell and Wallace*, 1992; *Wang and Wang*, 1999]. We report initial results of tropical Pacific changes in a coupled model to interhemispheric thermal gradient changes.

2. Model and Simulations

[3] Our model couples the Community Climate Model version 3.6 (CCM3) [*Kiehl et al.*, 1996] to a 1.5 layer reduced gravity ocean (RGO) model. A mixed layer is embedded in the upper layer of the RGO to simulate variations in SST, and the entrained subsurface temperature is tied to the simulated thermocline depth using a multivariate linear relationship. The model realistically simulates both the annual cycle and variability of SST, and has successfully been used in studies of tropical ocean-atmosphere variability [e.g., *Chang et al.*, 2007]. Our model differs from previous configurations in that full fluxes are now passed across the atmosphere-ocean boundary, rather than anomalous fluxes; also, the RGO domain is extended up to 80°N and S. More model details can be found in the auxiliary material[1].

[4] We run 50-year simulations, varying the strength of the interhemispheric gradient with a uniform surface flux forcing on all ocean gridpoints poleward of 40°N, at various levels from 30 W/m^2 warming to a 50 W/m^2 cooling; and a compensating flux south of 40°S, so that no net heat goes into the ocean. An anomalous interhemispheric thermal gradient develops, permeating into the tropics and driving a cross-equatorial flow that shifts the ITCZ to the warmer hemisphere (Figure 1). We define an index of the Pacific interhemispheric gradient as the difference between the SST averaged over 5°N–35°N and 120°E–240°E, with 5°S–35°S and 150°E–270°E.

3. Equatorial Pacific Zonal SST Gradient and Annual Cycle

[5] With a positive (warmer northern hemisphere (NH), cooler southern hemisphere (SH)) change to the interhemispheric gradient, the equatorial Pacific zonal SST gradient becomes steeper (Figure 2a, circles), primarily from an earlier onset and later retreat of the cold tongue that both prolongs and intensifies its cold phase (Figure 3a). Interestingly, it resembles the monthly climatological relationship between the zonal and interhemispheric SST gradients, provided the zonal SST gradient is lagged by one month from the interhemispheric SST gradient (Figure 2a, crosses).

[6] *Mitchell and Wallace* [1992] argued that the onset of the cold tongue is associated with increased southerlies in the eastern equatorial Pacific that initiates upwelling over the coastal zone. The cooling is transmitted to the equatorial interior through a coupled interaction between equatorial easterlies and SST: forced anomalous equatorial easterlies are generated to the west of the cold equatorial SST anomaly, driving both upwelling and increased evaporation that extends the cold anomaly further westward [*Nigam and Chao*, 1996]. This view is supported by theoretical and modeling studies [*Chang*, 1996; *Xie*, 1994] that show, in particular, that the cold tongue annual cycle originates from the annual cycle of the cross-equatorial flow.

[7] The model's response to changes in the interhemispheric gradient is consistent with this prevailing thinking.

---

[1]Department of Geography and Center for Atmospheric Sciences, University of California, Berkeley, California, USA.
[2]Department of Oceanography, Texas A&M University, College Station, Texas, USA.
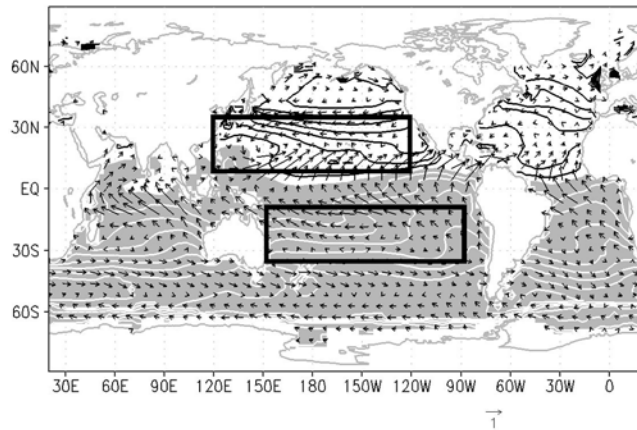
Figure 1. Model annual mean SST (contour interval 0.2 K, negative values are shaded, zero contour not plotted) and surface wind (vectors, reference vector is 1 m/s) response to interhemispheric forcing. The patterns are derived from linear regression of the model annual mean fields on the Pacific interhemispheric SST gradient (as defined in the text). The fields are in response to a 1°C increase to the annual mean interhemispheric gradient index. The boxes indicate the regions used to define this index.

With an anomalously warmer NH/cooler SH, the SST cooling in the far eastern Pacific starts earlier in the warm season (Figure 3a, blue shading), as does the westward propagation of the cold tongue and equatorial easterlies (Figure 3b). The anomalous northward-directed cross-equatorial flow (Figure 1) causes an earlier initiation of southerly trades off the coast of Peru (Figure 3c), driving coastal upwelling that initiates this sequence. The earlier cooling of the equatorial cold tongue comes about roughly equally through the easterlies' effect on increased upwelling and latent fluxes; the maintenance of the colder SST conditions in the middle of the cold period is due primarily to a similar cooling of subsurface waters that are entrained into the mixed layer (Figure 3d). This is due to a shallower equatorial thermocline tied to the increased equatorial easterlies throughout the cold season. This inference is supported by another set of simulations varying the interhemispheric gradient, but with the model's ocean modified so that the temperature of the subsurface waters was fixed to monthly climatological values; by doing so, ocean thermocline dynamics are not allowed to influence the SST. With these, the earlier westward propagation of colder SSTs is still present (indicating that it does not involve thermocline changes), but the SST cooling in the eastern Pacific in the latter half of the year is reduced. Consequently, changes in the annual mean zonal SST gradient to interhemispheric gradient changes are also reduced (Figure 2b).

[8] This reasoning suggests that the cold tongue annual cycle strength becomes larger with an increasingly positive interhemispheric gradient. This occurs in the eastern equatorial Pacific (Figure 2c, triangles), except for the largest positive interhemispheric gradients where the strength starts decreasing. By comparison, the equatorial western Pacific annual cycle strength (Figure 2c, crosses) remains muted for all simulation cases. The most interesting changes occur in
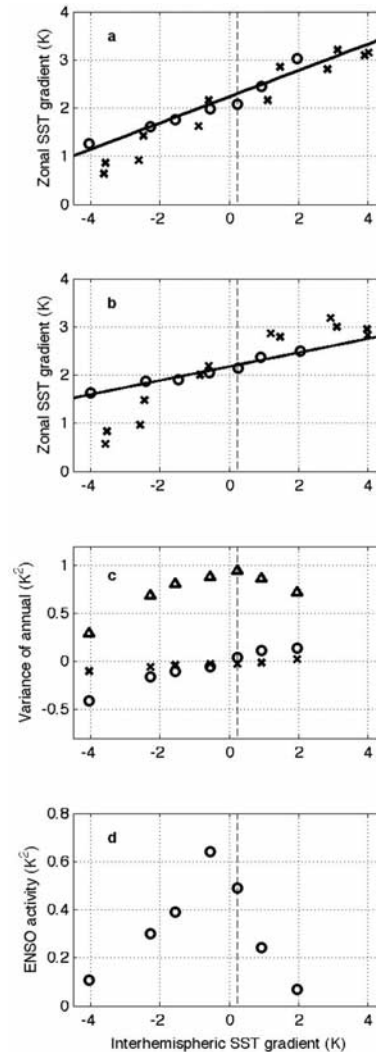
Figure 2. (a) Annual mean equatorial zonal SST gradient plotted as a function of the annual mean interhemispheric gradient index, for the various simulations (circles; solid line is the least square fit regression). The zonal SST gradient is defined to be the SST averaged over 5°N−5°S and 130°E to 200°E, subtracted from the SST averaged over 5°S−5°N and 200°E−270°E. Crosses are the same quantities, but for the climatological monthly mean relationship from the model, and with the zonal SST gradient lagged by one month from the interhemispheric gradient. (b) Same as Figure 2b, but using the simulations where the subsurface temperatures have been fixed to climatology. (c) Variance of the annually-varying component of equatorial SST plotted for the western Pacific (crosses; 130°E−180°E, 5°S−5°N); central Pacific (circles; 180°E−220°E, 5°S−5°N); and eastern Pacific (triangles; 220°E−270°E, 5°S−5°N). The sign is positive if the Mar−May temperatures are larger than Sep−Nov temperatures. The annual cycle is obtained from an ensemble empirical mode decomposition [*Wu and Huang*, 2008] to the 50-year long monthly mean cold tongue index. (d) ENSO activity as a function of the annual mean interhemispheric SST gradient. ENSO activity is computed as the variance of monthly mean Niño3 anomalies (SSTs averaged over 5°S−5°N, and 210°E−270°E). In all panels, the vertical dashed line is the interhemispheric gradient value for the control simulation.
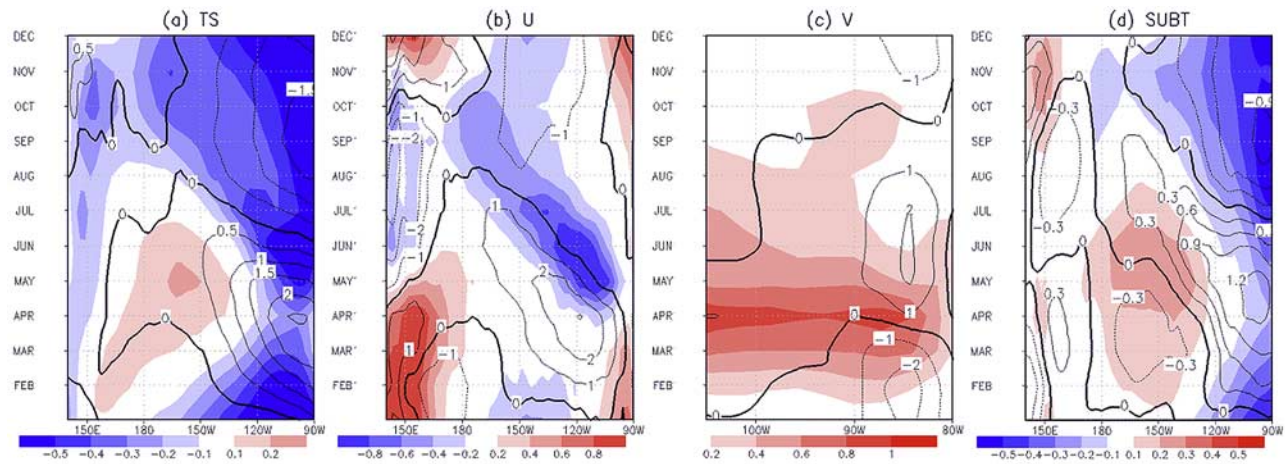
Figure 3. Change to the equatorial Pacific annual cycle with the interhemispheric SST gradient, shown as a Hovmoller diagram over Jan–Dec, and with longitude. In each of the 4 cases, monthly mean fields have been linearly regressed against the annual mean interhemispheric gradient index across the various perturbation simulations. The changes shown are in response to 2°C increase in this index. In all cases, the climatological seasonal cycle (i.e., annual mean is subtracted out) is shown in contours for reference; the zero contour is the thick line. (a) Equatorial SST (averaged over 5°S–5°N; scale units are in K), showing the earlier onset and later retreat of the cold phase of the eastern Pacific SST cycle. (b) Equatorial zonal wind (averaged over 5°S–5°N, scale units are m/s), showing the earlier boreal spring initiation of stronger equatorial easterlies. (c) Meridional wind speed just south of the equator (averaged over 14°S–5.5°S; scale units are m/s), likewise showing the earlier initiation of strong southerly trades near the coast in boreal spring. (d) Temperature of the subsurface waters entrained into the mixed layer (averaged over 5°S–5°N).

the equatorial central Pacific where the annual cycle phase reverses when the interhemispheric gradient changes from negative to positive (Figure 2c, circles). This is the focus of the next section.

4. Reversal of the Annual Cycle in the Central Equatorial Pacific

[9] The phase of the cold tongue annual cycle follows the southern hemisphere, a fact that *Wang and Wang* [1999] argues comes from (1) the existence of the colder equatorial SST, that allows for a bistable-state asymmetry to the eastern Pacific climate and (2) northward bias in the ITCZ. The observed climatological tropical interhemispheric SST gradient peaks (warm NH, cool SH) around Aug–Sep, a few months after the NH summer solstice because of the delayed response of the ocean mixed layer. Consequently, southeasterly trades impinging on the equator peak during this time, and the increased equatorial upwelling and evaporative cooling bring about a minimum in the cold tongue SST. This cooling reinforces the interhemispheric SST gradient, and helps lock the ITCZ in the north even as the northern hemisphere goes into wintertime. During the March equinox, the north–south gradient weakens but since the ITCZ is still to the north, the equatorial trades are at a minimum and hence the cold tongue SST is warmest.

[10] This hypothesis dictates that as the current northward ITCZ bias reverses with the imposition of anomalous interhemispheric gradients, the cold tongue annual cycle should *reverse*. This happens in our simulations, for the central Pacific (Figure 4a) – the warm season shifts abruptly from the March–May period to the Oct–Dec period, when the interhemispheric gradient reverses direction. The seasonality of the maximum trades on the equator shifts

with the switch of the ITCZ hemisphere as suggested by *Wang and Wang* [1999]: for a positive interhemispheric gradient, the strongest winds occur when the northeasterly
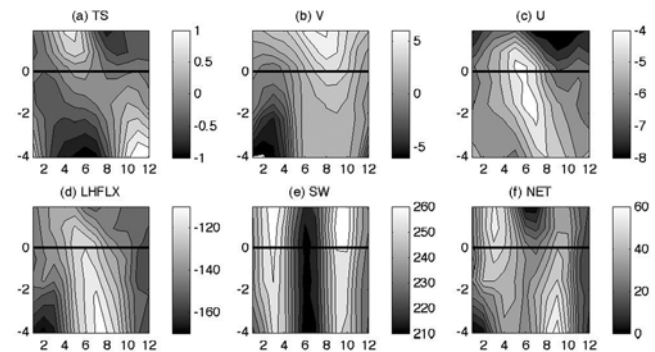
Figure 4. Changes to the seasonal cycle of the central equatorial Pacific with the interhemispheric SST gradient. The plotted quantities are averages over the 5°S–5°N, 180°E to 220°E region. The x-axis is the month of the year, and y-axis the interhemispheric SST gradient. (a) SST (K), with the yearly mean has been removed to emphasize the seasonal cycle, showing the reversal of the SST seasonal cycle as the interhemispheric gradient is reversed. (b) Meridional wind (m/s), showing the reversal in the cross-equatorial flow with the reversal of the interhemispheric gradient. (c) Zonal wind (m/s), showing the strongest anomalous westerlies in the Apr–May period for the strongest positive interhemispheric SST gradient, gradually shifting to Aug–Sep for the strongest negative gradients. (d) Latent heat flux (W/m²), with phasing controlled by the zonal winds. (e) Net shortwave flux (W/m²) with a biannual signal. (f) Net surface flux (W/m²). For Figures 4d–4f, positive flux is downwards.

trades impinge on the central equatorial Pacific in Jun–Sep; whereas for a negative gradient, it is Jan–Apr (Figures 4b and 4c). Consequently, the latent heat flux (Figure 4d) is at a minimum prior to the cold tongue warm season.

[11] The latent flux changes, being gradual, alone cannot explain the abrupt switch to the SST phase; rather, it results from the combination of latent flux and net shortwave flux, the two largest controls of the central equatorial Pacific SST. Net shortwave peaks during the equinoxes (Figure 4e), so the latent flux changes acts with the shortwave flux when the interhemispheric gradient are at the extremes, but against it when the interhemispheric gradient is small (Figure 4f). Thus, the SST annual cycle abruptly shifts in phase even though the changes to the latent flux are gradual.

[12] The reversal of the equatorial annual cycle occurs only in the central Pacific; further east, the annual cycle is maintained in the same sense as for the present-day climate, though it weakens as the interhemispheric SST gradient becomes more negative (Figure 2c). A plausible hypothesis for this difference is that the cold tongue is weaker in the central equatorial Pacific and cannot maintain a northward-biased ITCZ in the face of a sufficiently negative interhemispheric gradient forcing. On the other hand, the cooler SST in the southeastern Pacific relative to its northern counterpart is thought to be determined by the coastal southeast to northwest geometry (and hence fixed), given that only southeasterly trades can initiate cooling there [*Philander et al.*, 1996].

5. ENSO Activity

[13] For completeness, we briefly report a strong sensitivity of the model ENSO activity to interhemispheric gradients. Changes to ENSO are most commonly thought to arise through changes in the mean state [e.g., *Tziperman et al.*, 1997], though changes in the stochastic forcing of ENSO may also factor [e.g., *Chang et al.*, 2007]. ENSO activity peaks when the absolute north–south meridional SST gradient is close to zero, and reduces sharply as the gradient increases in either direction (Figure 2d). Interestingly, the control simulation interhemispheric gradient (that most closely approximates present-day climate) is around 0.23 K, and resides in a sensitive region of ENSO change.

[14] We defer the analysis of the mechanisms of ENSO change to upcoming studies, though we briefly mention consistency of these results to our recent analysis of 20th century changes in ENSO activity [*Fang et al.*, 2008]. The pattern of global SST that *Fang et al.* [2008] found to be associated to 20th century ENSO variance has an interhemispheric gradient character, with cooler northern ocean SST anomalies during times of higher ENSO activity, consistent with the results of this study.

6. Discussion

[15] Our results are subject to limitations in the model's ocean dynamics: first, we do not model subsurface variations in ocean temperature due to advective effects that may be influential in tropical Pacific climate change [*Gu and Philander*, 1997]. Second, the flux correction applied to the ocean may impact the manner in which the tropical Pacific responds to the interhemispheric forcing. In applying a flux correction, we decided that a more realistic basic state was more important than the limitations imposed by it. There is also the more general issue of how dependent these results are to the model used. Regardless, our results amply demonstrate that the tropical Pacific coupled climate is sensitive to changes in the interhemispheric gradient, and in a nontrivial fashion.

[16] The pertinent next question is whether or not changes to the interhemispheric gradient can be usefully applied to understand tropical Pacific changes in paleoclimate scenarios. An obvious candidate is the Last Glacial Maximum (LGM) climate, where the hemispheric asymmetric distribution of land ice – heavily favoring the north – provides the interhemispheric gradient forcing [e.g., *Manabe and Broccoli*, 1985].

[17] *Timmermann et al.* [2007] have analyzed the tropical Pacific climate changes to Atlantic Meridional Overturning circulation (AMOC) slowdown in several coupled models using the interhemispheric gradient concept. NH cooling due to AMOC slowdown causes a reduction to the interhemispheric gradient towards a more symmetric state: as a consequence, they found (in 4 of 5 models examined) that the cold tongue annual cycle amplitude decreases, and ENSO variance increases. Our results are qualitatively consistent with *Timmermann et al.* [2007] for both the cold tongue annual cycle and ENSO variance; the exception is the annual cycle of SST in the far eastern equatorial Pacific, whose amplitude does not change much (see Figure 2c, triangles). Nevertheless, our results support the contention by Timmermann et al. that the AMOC slowdown influence on the tropical Pacific arises through the changed interhemispheric gradient.

[18] We are intrigued by the suggestion of a mechanism for abrupt change for the tropical Pacific, since a convincing tropical mechanism for abrupt climate change has yet to be proposed that matches the AMOC in stature [*Broecker*, 2003]. A prior reversal of the interhemispheric gradient is required for this to be a viable mechanism for abrupt climate changes – but how this reversal can be initiated, is unclear. Nevertheless, a more comprehensive study of this, with a fully coupled model, is clearly of interest.

References

Broccoli, A. J., K. A. Dahl, and R. J. Stouffer (2006), Response of the ITCZ to Northern Hemisphere cooling, *Geophys. Res. Lett.*, *33*, L01702, doi:10.1029/2005GL024546.

Broecker, W. S. (2003), Does the trigger for abrupt climate change reside in the ocean or in the atmosphere?, *Science*, *300*, 1519–1522.

Chang, P. (1996), The role of the dynamic ocean-atmosphere interactions in the tropical annual cycle, *J. Clim.*, *9*, 2973–2985.

Chang, P., L. Zhang, R. Saravanan, D. J. Vimont, J. C. H. Chiang, L. Ji, H. Seidel, and M. K. Tippett (2007), Pacific meridional mode and El Niño—Southern Oscillation, *Geophys. Res. Lett.*, *34*, L16608, doi:10.1029/2007GL030302.

Chiang, J. C. H., and C. M. Bitz (2005), Influence of high latitude ice cover on the marine Intertropical Convergence Zone, *Clim. Dyn.*, *25*, 477–496.

Fang, Y., J. C. H. Chiang, and P. Chang (2008), Variation of mean sea surface temperature and modulation of El Niño–Southern Oscillation variance during the past 150 years, *Geophys. Res. Lett.*, *35*, L08703, doi:10.1029/2007GL033097.

Gu, D. F., and S. G. H. Philander (1997), Interdecadal climate fluctuations that depend on exchanges between the tropics and extratropics, *Science*, *275*, 805–807.

Kiehl, J. T., et al. (1996), Description of the NCAR community climate model, NCAR Tech. Note 152, Natl. Cent. for Atmos. Res., Boulder, Colo.

Koutavas, A., and J. Lynch-Stieglitz (2004), Variability of the Marine ITCZ over the eastern Pacific during the past 30,000 years, in *The Hadley Circulation: Past, Present, and Future*, *Adv. Global Change Res.*, vol. 21, edited by H. F. Diaz and R. Bradley, pp. 347–369, Springer, New York.

Manabe, S., and A. J. Broccoli (1985), The influence of continental ice sheets on the climate of an ice-age, *J. Geophys. Res.*, *90*, 2167–2190.

Mitchell, T. P., and J. M. Wallace (1992), The annual cycle in equatorial convection and sea-surface temperature, *J. Clim.*, *5*, 1140–1156.

Nigam, S., and Y. Chao (1996), Evolution dynamics of tropical ocean-atmosphere annual cycle variability, *J. Clim.*, *9*, 3187–3205.

Philander, S. G. H., et al. (1996), Why the ITCZ is mostly north of the equator, *J. Clim.*, *9*, 2958–2972.

Timmermann, A., et al. (2007), The influence of a weakening of the Atlantic meridional overturning circulation on ENSO, *J. Clim.*, *20*, 4899–4919.

Tziperman, E., S. E. Zebiak, and M. A. Cane (1997), Mechanisms of seasonal–ENSO interaction, *J. Atmos. Sci.*, *54*, 61–71.

Wang, B., and Y. Q. Wang (1999), Dynamics of the ITCZ-equatorial cold tongue complex and causes of the latitudinal climate asymmetry, *J. Clim.*, *12*, 1830–1847.

Wu, Z., and N. E. Huang (2008), Ensemble empirical mode decomposition: A noise assisted data analysis method, *Adv. Adaptive Data Anal.*, in press.

Xie, S.-P. (1994), On the genesis of the equatorial annual cycle, *J. Clim.*, *7*, 2008–2013.

—————————————

P. Chang, Department of Oceanography, Texas A&M University, College Station, TX 77843, USA.

J. C. H. Chiang and Y. Fang, Department of Geography and Center for Atmospheric Sciences, University of California, Berkeley, CA 94720–4740, USA. (jchiang@atmos.berkeley.edu)